Int J Adv Manuf Technol (2004) 23: 87–92
DOI 10.1007/s00170-003-1556-7

ORIGINAL ARTICLE

Jae-Seob Kwak · Man-Kyung Ha

Detection of dressing time using the grinding force signal based on the discrete wavelet decomposition

Received: 31 July 2002 / Accepted: 7 October 2002 / Published online: 22 November 2003

Abstract This paper describes the use of the grinding force signal to show the mechanical noise reduction and to detect the dressing time based on the discrete wavelet decomposition. As a result of de-noising, the wavelet de-noising method was more effective than the FFT filtering technique. From the approximation coefficients of the higher order wavelet transform, the grinding force signal obtained by a tool dynamometer was clear so it was possible to successfully detect the dressing time. A measured result by the surface roughness and the ground surface photograph coincided with the detection result.

Keywords Grinding force · Discrete wavelet decomposition · De-noising method · Dressing time

1 Introduction

Numerous promotions of manufacturing systems have been observed over the last few decades. The core of these promotions, especially the machining process, is a manufacturing system which is based upon the automatic operation where there is no man power necessary. Accordingly, in an automatic manufacturing system, it is more important to monitor lastingly the machining state, which always continues as a stable state without an unexpected fault such as breakage of tools, malfunctioning of the machine, product quality and grinding wheel loading.

The grinding force usually reflects the working condition of the machine. The accuracy of the grinding process is affected by various factors for example wheel speed, feed, depth of the cut, the dressing condition and the dull cutting edge. In the grinding process, like other machining processes, the topography of the grinding wheel has a direct relationship with the ground surface [1,2]. Various techniques are used to examine the integrity of a ground surface, to monitor the grinding process itself, or to evaluate the grinding wheel life.

A lifting wavelet model for enhancement of accuracy of surface roughness characterisation was proposed by Jiang et al. [3]. In this work, the theory and fast algorithm of the lifting wavelet were briefly introduced and the lifting wavelet model for extraction of roughness of surfaces had been developed. The rough surface recovered had good refinement accuracy in contrast to the least squares polynomial fitting. Lin [4] used a de-noising method based on the Morlet wavelet in acoustic signals. When this method was applied to the sound extraction, it could be seen to be very effective. Lee and Tarng [5] described the use of induction motor current to detect the occurrence of drill fracture based on the discrete wavelet transform. The scaling and shifting coefficients in the discrete wavelet transform were chosen as powers of tow so that a multi-level signal decomposition of the induction motor current could be performed.

Nowadays, a precision machining of aluminium alloy, copper alloy, stainless steel and titanium has been required very much in the scope of many industries. Conventionally, the grinding of these materials is difficult because of the mechanical properties such as low hardness and high toughness which result in the wheel loading and poor surface integrity. Because the final precision machining of these kinds of materials mainly depends on cutting method, it is difficult to obtain higher machining accuracy and better surface roughness [6]. A new grinding wheel had been developed by Yamaguchi et al. [7], wherein very fine SiC whiskers were aligned normally to the grinding surface. However, the grinding wheel exhibited a tendency toward loading. The loading of the grinding wheel could be remarkably reduced by the addition of a small amount of very fine abrasive grains to the grinding fluid. Nevertheless, the loading of the grinding wheel is a big matter avoided in the

J.-S. Kwak (✉) · M.-K. Ha
School of Mechanical Engineering,
Pukyong National University, San 100,
Yongdang-dong, Nam-Ku,
608-739 Busan, S. Korea
E-mail: jskwak5@pknu.ac.kr

grinding. In a case of the wheel loading, it is possible to prescribe the loaded wheel for redressing [8,9]. However, because prevention is better than cure, the correct detection of the wheel loading is more important.

In this study, a wavelet transform technique was applied to a feature extraction and a de-noising of the grinding force signal obtained from a tool-dynamometer. As a result of the wavelet application, the redressing needed time due to the wheel loading in a grinding wheel and the onset points of a chatter vibration could be detected.

2 Wavelet decomposition

2.1 Review of wavelet transform

The wavelet transform is a popular tool for studying intermittent and localised phenomena in various signals. Due to the multi-resolution ability of a wavelet transform, the noised signals can be separated into several approximation signals and detail signals [5]. The wavelet transform of a signal $f(t)$ is defined as the sum of all of the time of the signal $f(t)$ multiplied by a scaled and shifted version of the wavelet function $\Psi(t)$. The coefficients $C(a,b)$ of the wavelet transform of the signal $f(t)$ can be expressed as follows.

$$C(a,b) = \int_{-\infty}^{\infty} f(t) a^{-0.5} \Psi\left(\frac{t-b}{a}\right) dt \tag{1}$$

Where a and b are the scaling and shifting parameters in the wavelet transform. Basically, a small scaling parameter corresponds to a compressed wavelet function. Therefore, the high frequency features in the signal $f(t)$ can be obtained from the wavelet transform by using a small scaling parameter. On the other hand, the low frequency feature can be extracted by using a large scaling parameter with a stretched wavelet function.

For the sampled signal $f(k)$, a discrete wavelet transform can be used. The most commonly used discrete wavelet transform is the scaling and shifting of parameters with powers of two.

$$a = 2^j \tag{2}$$

$$b = ka = k2^j \tag{3}$$

Where j is the number of levels in the discrete wavelet transform. The coefficients $C(a,b)$of the discrete wavelet transform can be divided into two parts. One is the approximation coefficients and the other is the detailed coefficients. The approximation coefficients are the high scale and the low frequency components of the signal $f(t)$, while the detail coefficients are the low scale and the high frequency components of the signal $f(t)$. The approximation coefficients (A_j) of the discrete wavelet transform for the sampled signal $f(t)$ at level j can be expressed as Eq. 4.

$$A_j = \sum_{n=0}^{\infty} f(n)\psi_{j,k}(n) = \sum_{n=0}^{\infty} f(n) \frac{1}{\sqrt{2^j}} \psi\left(\frac{n-k2^j}{2^j}\right) \tag{4}$$

Where $\Psi_{j,k}(n)$ is the scaling function associated with the wavelet function $\Psi_{j,k}(n)$. Similarly, the detail coefficients (D_j) of the discrete wavelet transform for the sampled signal $f(t)$ at level j can be expressed as follows.

$$D_j = \sum_{n=0}^{\infty} f(n)\Psi_{j,k}(n) = \sum_{n=0}^{\infty} f(n) \frac{1}{\sqrt{2^j}} \Psi\left(\frac{n-k2^j}{2^j}\right) \tag{5}$$

From Eqs. 4 and 5, the decomposition of the signal $f(k)$ can be iterated as the number of levels increases. As a result, a hierarchical set of approximation coefficients and detail coefficients can be obtained through the multi-level signal decomposition. Useful information for the signal $f(t)$ can then be yielded from the multi-level wavelet signal decomposition. As shown in Fig. 1, a wavelet decomposition tree with three levels can be made through this transformation process. The original signal $f(t)$ can be split into an approximation A_1 and a detail D_1. Then, the approximation A_1 is also split to obtain a second level approximation A_2 and detail D_2. This process continues to arrive at the j level. In this study, the forth level were used for detecting the grinding wheel loading.

2.2 De-noising technique

The wavelet expansions tend to concentrate the data energy into a relatively small number of large coefficients. This energy concentration property of the wavelet transform makes the wavelet domain appropriate for signal estimation. Nonlinear wavelet shrinkage methods can be divided into the hard threshold filter and the soft threshold filter.

(a) Hard threshold filter

$$\begin{aligned} f_{\text{hard}}(t) &= f(t), \quad \text{if } f(t) > \delta \\ &= 0, \quad \text{if } f(t) \le \delta \end{aligned} \tag{6}$$

(b) Soft threshold filter

$$\begin{aligned} f_{\text{soft}}(t) &= \text{sign}(f(t))(|f(t)| - \delta), \quad \text{if } f(t) > \delta \\ &= 0, \quad \text{if } f(t) \le \delta \end{aligned} \tag{7}$$

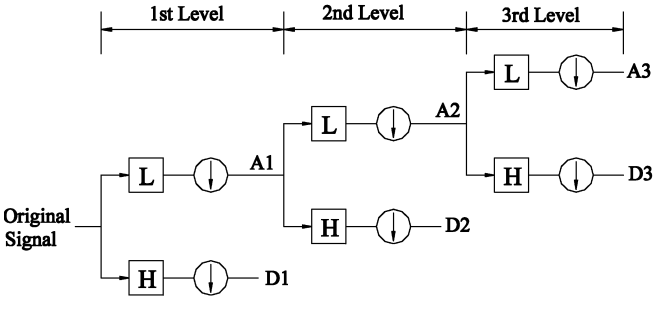

Fig. 1 Wavelet decomposition tree with three levels

Where δ is a threshold and presented as

$$\delta = \sqrt{2\log(n)}2\sigma n^{-0.5}2^{(J-j)/2} \quad (8)$$

Where n is the number of samples, σ is a noise standard deviation and J are scale coefficients.

This type of a signal de-noising method was found to be very effective for suppressing noises. The method is very different from traditional linear methods of smoothing, which achieve noise suppression only by significantly broadening and erasing certain features. An example of de-noising with a wavelet and the FFT filter was illustrated in Fig. 2.

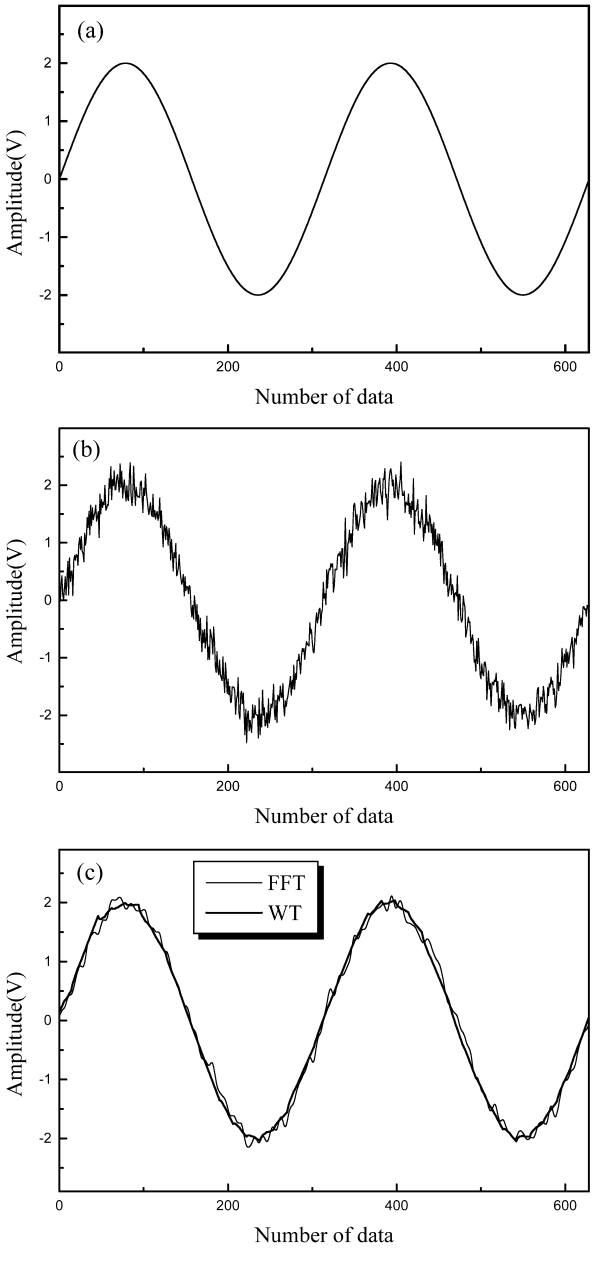

Fig. 2 An example of signal de-noising. **a** Original signal **b** Noised signal **c** De-noising signals

A given signal has a sinusoid curve shown in Fig. 2a. The amplitude and the period of this signal are 2 V and 314 sample data respectively. Figure 2b presents the signal including a random data set as a signal noise. This is a small different signal profile as compared with the original signal shown in Fig. 2a. Figure 2c plotted the results of de-noising signals using the FFT filtering and the wavelet de-noising.

It was evident that the fine noised components of the original signal remained clear after the de-noising. The result of the wavelet de-noising was more similar to the original signal than that of the FFT filtering. Therefore, it seen that the wavelet method could be efficiently used in the de-noising of the grinding force signal.

3 Experimentation

Figure 3 presents the schematic experimental set-up to obtain the grinding force signal in surface plunge grinding. A grinding wheel of the WA type was used and the specimen was STD11. A tool dynamometer (Kistler, 9257B) was fastened on the magnetic chuck.

During the grinding operation, obtained grinding force signals were transferred into a charge amplifier (Kistler, 5019) and then analogue signals passing the amplifier were converted to digital data by an A/D converter. The data were saved in a personal computer and used to the wavelet decomposition. The grinding wheel revolution was 1,800 rpm. The table speed was 4 m/min and the depth of a cut was 10 μm. Table 1 listed the grinding conditions.

4 De-noising grinding force signals

Figure 4a shows a typically measured grinding force signal during one cycle. It is the sum of a grinding force and a noised signal so it is difficult to understand the magnitude and the tendency of the grinding force change. It is necessary to remove the noise.

The FFT method, which has been used sometimes as a de-noising technique, simply smoothes the noised data. The smoothing is accomplished by removing Fourier

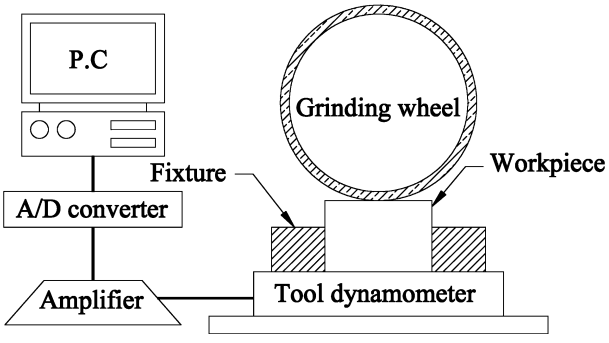

Fig. 3 Experimental set-up to obtain the grinding force signal

Table 1 Experimental conditions

Items	Conditions
Spindle speed	1,800 rpm
Grinding method	Plunge, wet and down grinding
Grinding wheel	WA100L mV
Specimen	STD11
Table speed	4 m/min
Depth of cut	10 μm
Cutting fluid	Shell lubricant (20:1)

components with frequencies higher than $1/(n\times\Delta t)$ where n is the number of data points considered at a time, and Δt is the time (or more generally the abscissa) spacing between two adjacent data points. Therefore, the result of the FFT process goes wrong as compared with the original data. For the sake of the reformation of a defect in the FFT method, the wavelet de-noising method can be used.

Figure 4b presents the results of the FFT filtering and the wavelet de-noising. It is seen that the grinding force profile is very clear and easy to analyse the characteristics. In this case, the grinding force level changes widely from 5 N to 15 N. In comparison with the results, the wavelet de-noising is very similar to the FFT filtering. Now the grinding system is in an unstable condition and the related parameter should be changed. Therefore, it is seen that the wavelet de-noising method is very useful when the de-noising of the grinding force signal is applied.

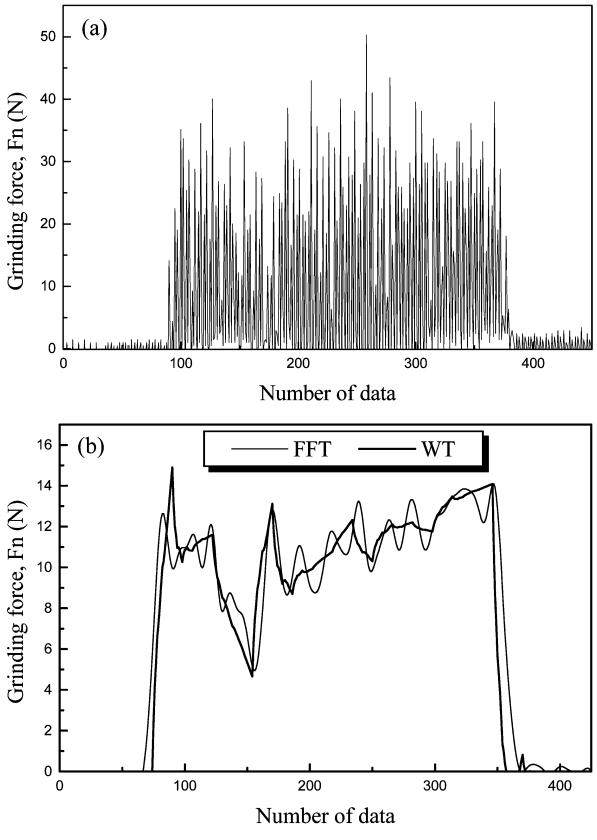

Fig. 4 Comparison between wavelet de-noising and FFT in one-cycle grinding force signal. **a** Measured grinding force signal **b** De-noised grinding force signal

5 Detection of wheel loading

In order to detect the dressing time of a grinding wheel through the analysis of the grinding force signal, the experiment was continued. Figure 5 shows the obtained grinding force signal according to the number of machined pieces. As shown in Fig. 5, the grinding force increased linearly with an increasing number of machined pieces from initiation to the 45th piece. After the 45th piece, the grinding force level decreased but it fluctuated severely. This was because cutting edges in the grinding wheel were dulling gradually and the voids between the abrasive grains were filled with adhesive materials during the cutting operation so the grinding operation was not peaceful. Therefore, the grinding force was increased before 45th piece.

The critical limit of the useful operation in this wheel was at about the 45th piece, which was the dressing time in a practical case. After the dressing time (wheel life), the grinding wheel had a self-redressing process so the grinding force level decreased. However, this is not homogeneous in all of the abrasive edges. It induces the oscillation of the grinding wheel during the machining. Although the grinding force level is lower, these times are unstable for grinding.

To detect the dressing time clearly, the discrete wavelet transform used Daubechies wavelets because the Daubechies wavelets were suitable for the detection of a sudden signal change at the time or frequency domain. Figure 6 shows the result of the first level wavelet decomposition in 85 grinding cycles. In the approximation coefficients A_1, it had a peak level at about the 45th piece which is the same as in Fig. 5. The detail coefficients D_1 were shown in Fig. 6b. It was difficult to detect the dressing time with the first level wavelet decomposition. Therefore a higher order of the Daubechies wavelet was conducted.

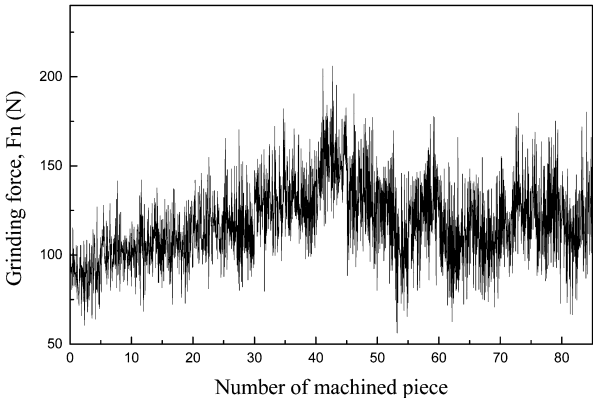

Fig. 5 Obtained grinding force signals without dressing

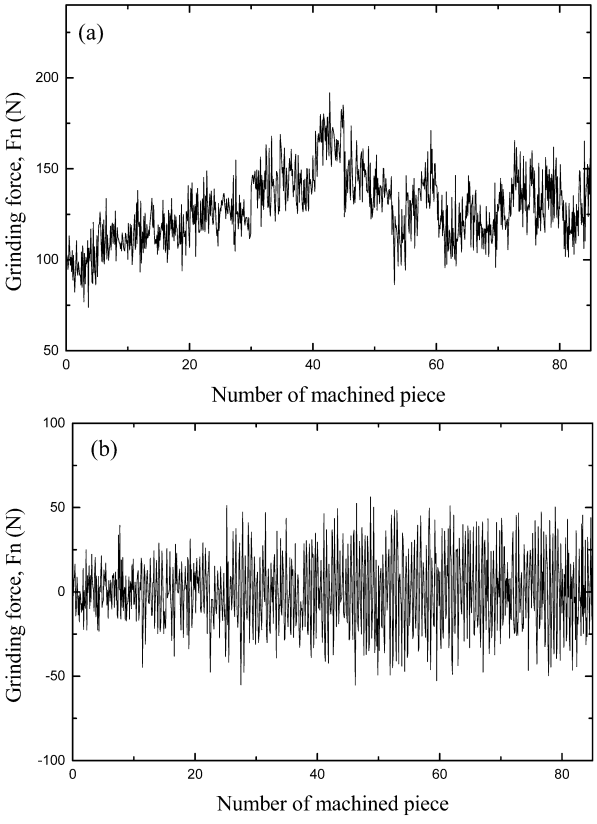

Fig. 6 First level wavelet transform in grinding force signals. **a** Approximation coefficients A1 **b** Detail coefficients D1

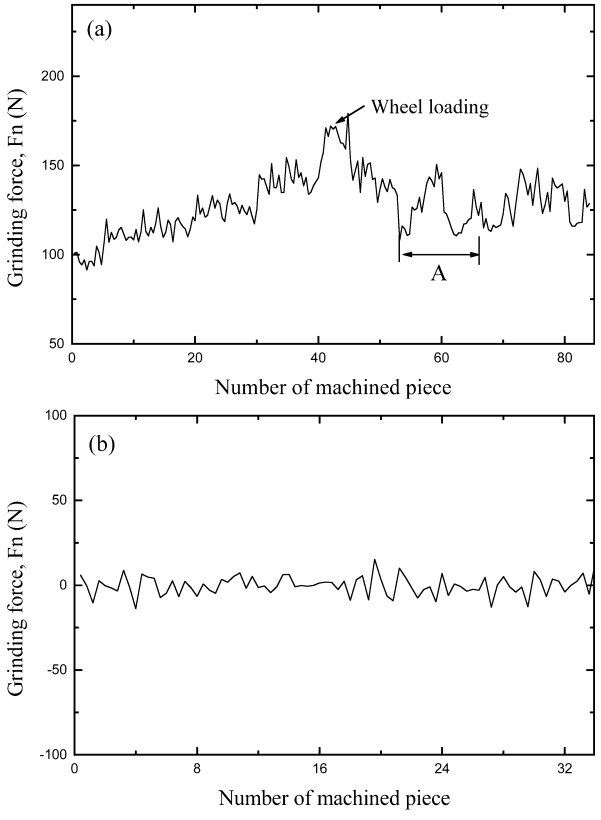

Fig. 7 Forth level wavelet transform in grinding force signals. **a** Approximation coefficients A4 **b** Detail coefficients D4

Figure 7 presents the result of the forth level wavelet decomposition. The approximation coefficients A_4 clearly give the decision of the dressing time that is needed. Also, after the dressing time, the chatter vibration was confirmed at the unstable region marked A in Fig. 7a. These results demonstrate the effectiveness of the wavelet application in the grinding operation.

Figure 8 presents the result of a measured surface roughness according to the number of machined pieces. The surface roughness was plotted as an average value and a deviation. As shown in Fig. 8, the surface roughness increased greatly after the 40th piece and the deviation was wide. Because the specimen STD11 was comparatively a ductile material, it was seen that the grinding wheel was loaded with adhesive materials.

From these results, after the 40th piece the redressing of the grinding wheel was required. This was the wheel life and it coincided with the result of the wavelet decomposition shown in Fig. 7.

Figure 9 shows a photograph of the ground surface at the time occurring the chatter vibration presented by a character **A** in Fig. 7a. The grinding direction is horizontal. The chatter marks, which are normal to the grinding direction, are shown. Therefore, it is important to detect the wheel loading and to conduct the redressing grinding operation in order to ensure a good ground surface quality.

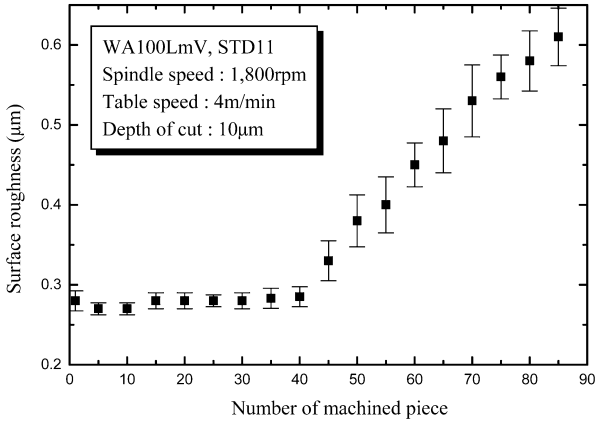

Fig. 8 Surface roughness variation according to the number of machined pieces

6 Conclusion

In this study, the discrete wavelet decomposition was introduced and applied to the grinding process. The possibility of de-noising through the discrete wavelet decomposition was examined with a random noised sinusoid signal. In the de-nosing method of the wavelet technique, the results were compared to that of the FFT

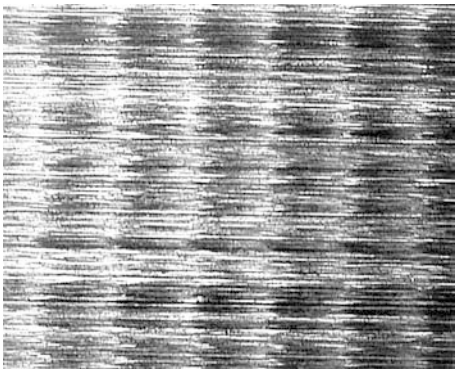

Fig. 9 Photograph of the ground surface occurring chatter vibration

filtering. These results were very similar to each other but the wavelet de-noising was nearer to the original signal.

In the grinding process, the time at which a grinding wheel was necessary to redress because the corrective grinding operation was impossible was determined with the wavelet technique. The grinding force according to the number of machined pieces increased when the redressing was needed. Also, the surface roughness deteriorated at the wheel loading. The chatter marks were observed on the ground surface.

When a higher level of the wavelet deposition was applied, the easiest detection of the redressing time was made in a processed signal. From the result of this study, it was seen that the wavelet transform technique was very powerful and that it had unlimited application potential.

References

1. Wang YW, Moon KS (1997) A methodology for the multi-resolution simulation of grinding wheel surface. Wear 211(11):218–225
2. Kwak JS, Song JB (2001) Trouble diagnosis of the grinding process by using acoustic emission signals. Int J Mach Tools Manuf 41(3):899–913
3. Jiang XQ, Blunt L, Stout KJ (2001) Application of the lifting wavelet to rough surface. Precis Eng 25(2):83–89
4. Lin J (2001) Feature extraction of machine sound using wavelet and its application in fault diagnosis. MDT & E Int 34(1):25–30
5. Lee BY, Tarng YS (2000) Drill facture detection by the discrete wavelet transform. J Mater Process Technol 99(3):250–254
6. Kim JD, Kang YH, J DX, Lee YS (1997) Development of discontinuous grinding wheel with multi-porous grooves. Int J Mach Tools Manuf 37(11):1611–1624
7. Yamguchi K, Horaguchi I, Sato Y (1998) Grinding with directionally aligned SiC whisker wheel-loading free grinding. Precis Eng 22(2):59–65
8. Zhang C, Shin YC (2002) A novel laser-assisted truing and dressing technique for vitrified CBN wheels. Int J Mach Tools Manuf 42(7):825–835
9. Lim HS, Fathima K, Kumar AS, Rahman M (2002) A fundamental study on the mechanism of electrolytic in-process dressing (ELID) grinding. Int J Mach Tools Manuf 42(8):935–843